

RESEARCH OUTPUTS / RÉSULTATS DE RECHERCHE

Transformed-linear prediction for extremes

Lee, Jeongjin; Cooley, Daniel

Publication date:
2021

[Link to publication](#)

Citation for published version (HARVARD):

Lee, J & Cooley, D 2021 'Transformed-linear prediction for extremes'.

General rights

Copyright and moral rights for the publications made accessible in the public portal are retained by the authors and/or other copyright owners and it is a condition of accessing publications that users recognise and abide by the legal requirements associated with these rights.

- Users may download and print one copy of any publication from the public portal for the purpose of private study or research.
- You may not further distribute the material or use it for any profit-making activity or commercial gain
- You may freely distribute the URL identifying the publication in the public portal ?

Take down policy

If you believe that this document breaches copyright please contact us providing details, and we will remove access to the work immediately and investigate your claim.

Transformed-linear prediction for extremes

Jeongjin Lee*

Department of Statistics, Colorado State University
and

Daniel Cooley

Department of Statistics, Colorado State University

July 14, 2022

Abstract

We consider the problem of performing prediction when observed values are at their highest levels. We construct an inner product space of nonnegative random variables from transformed-linear combinations of independent regularly varying random variables. Under a reasonable modeling assumption, the matrix of inner products corresponds to the tail pairwise dependence matrix, which summarizes tail dependence. The projection theorem yields the optimal transformed-linear predictor, which has the same form as the best linear unbiased predictor in non-extreme prediction. We also construct prediction intervals based on the geometry of regular variation. We show that these intervals have good coverage in a simulation study as well as in two applications: prediction of high pollution levels, and prediction of large financial losses.

Keywords: Multivariate Regular Variation, Projection Theorem, Tail Pairwise Dependence Matrix, Air Pollution, Financial Risk

*Jeongjin Lee and Daniel Cooley were partially supported by US National Science Foundation Grant DMS-1811657.

1 Introduction

Prediction of unobserved quantities is a common objective of statistical analyses. Figure 1 shows the one-hour maximum measurements of the air pollutant nitrogen dioxide (NO_2) in parts per billion for four monitoring stations in the Washington DC area on January 23, 2020. Given these measurements, it is natural to ask what the predicted level would be at a nearby unmonitored location such as Alexandria VA, which is marked “Alx” in Figure 1 and which had NO_2 monitoring prior to 2015. What makes this particular day interesting is that measurements are at very high levels; each measurement exceeds its station’s empirical 0.98 quantile for the year, and the Arlington station (Arl) is recording its highest measurement for the year. We propose a linear prediction method which is designed specifically for when observed values are at extreme levels and which is based on a framework from extreme value analysis.

If the joint distribution of all variates were known, the conditional distribution would provide complete information about the variate of interest given the observed values. The air pollution data’s distribution is not known, is clearly non-Gaussian, and there is no clear choice for a candidate joint distribution. Further, extreme value analysis would caution against using a model that had been fit to the entire data set to describe behavior in the joint tail.

Linear methods, such as kriging in spatial statistics, offer a straightforward predictor by simply applying weights to each of the observations. Linear prediction methods do not require specification of the joint distribution and instead provide the best (in terms of mean square prediction error, MSPE) linear unbiased prediction (BLUP) weights given only the covariance structure between the observed and unobserved measurements. Uncertainty is often summarized by MSPE and prediction intervals are commonly based on

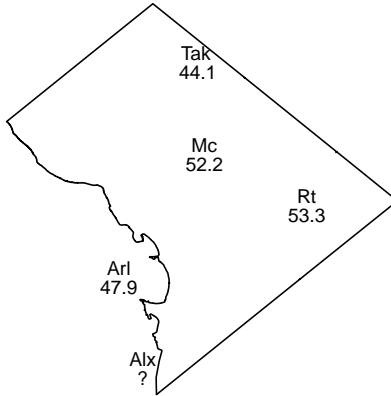


Figure 1: Maximum NO₂ measurements for January 23, 2020. All observations are above the empirical .98 quantile for each location.

Gaussian assumptions. However, covariance could be a poor descriptor of dependence in a distribution's joint upper tail, and Gaussian assumptions may be poorly suited to describe uncertainty in the tail.

In this work, we propose an extremal prediction method which is similar in spirit to familiar linear prediction. We will analyze only data which are extreme. To provide a framework for modeling dependence in the upper tail, we rely on regular variation on the positive orthant. Modeling in the positive orthant allows our method to focus only on the upper tail, which is assumed to be the direction of interest; in this example we are interested in predicting when pollution levels are high. On the way to developing our prediction method, we will construct a vector space of non-negative regularly-varying random vectors arising from transformed-linear operations. We summarize pairwise tail dependencies in a matrix which has properties analogous to a covariance matrix. Our transformed-linear predictor has a similar form to the BLUP in non-extreme linear prediction. Rather than being based on the elliptical geometry underlying standard linear prediction, uncertainty

quantification is based on on the polar geometry of regular variation. We will show that our method has good coverage when applied to the Washington air pollution data and also when applied to a higher dimensional financial data set.

2 Background

2.1 Regular variation on the positive orthant

Informally, a multivariate regularly varying random variable has a distribution which is jointly heavy tailed. Regular variation is closely tied to classical extreme value analysis (De Haan & Ferreira 2007, Appendix B), and Resnick (2007) gives a comprehensive treatment. Let \mathbf{X} be a p -dimensional random vector that takes values in $\mathbb{R}_+^p = [0, \infty)^p$. \mathbf{X} is regularly varying (denoted $RV_+^p(\alpha)$) if there exists a function $b(s) \rightarrow \infty$ as $s \rightarrow \infty$ and a non-degenerate limit measure $\nu_{\mathbf{X}}$ for sets in $[0, \infty)^p \setminus \{\mathbf{0}\}$ such that

$$sPr(b(s)^{-1}\mathbf{X} \in \cdot) \xrightarrow{v} \nu_{\mathbf{X}}(\cdot) \quad (1)$$

as $s \rightarrow \infty$, where \xrightarrow{v} indicates vague convergence in the space of non-negative Radon measures on $[0, \infty)^p \setminus \{\mathbf{0}\}$. The normalizing function is of the form $b(s) = U(s)s^{1/\alpha}$ where $U(s)$ is a slowly varying function, and α is termed the tail index.

For any set $C \subset [0, \infty)^p \setminus \{\mathbf{0}\}$ and $k > 0$, the measure has the scaling property $\nu_{\mathbf{X}}(kC) = k^{-\alpha}\nu_{\mathbf{X}}(C)$. This scaling property implies regular variation can be more easily understood in a polar geometry. Given any norm, $r > 0$, and Borel set $B \subset \mathbb{S}_{p-1}^+ = \{\mathbf{w} \in \mathbb{R}_+^p : \|\mathbf{w}\| = 1\}$, the set $C(r, B) = \{\mathbf{x} \in \mathbb{R}_+^p : \|\mathbf{x}\| > r, \mathbf{x}/\|\mathbf{x}\| \in B\}$ has measure $\nu_{\mathbf{X}}(C(r, B)) = r^{-\alpha}H_{\mathbf{X}}(B)$, where $H_{\mathbf{X}}$ is a measure on \mathbb{S}_{p-1}^+ . The angular measure $H_{\mathbf{X}}$ fully describes tail dependence in the limit; however, modeling $H_{\mathbf{X}}$ even in moderate dimensions is difficult. The measure's intensity function in terms of polar coordinates is $\nu_{\mathbf{X}}(dr \times d\mathbf{w}) = \alpha r^{-\alpha-1}drdH_{\mathbf{X}}(\mathbf{w})$.

2.2 Transformed linear operations

In order to perform linear-like operations for vectors in the positive orthant, Cooley & Thibaud (2019) defined transformed linear operations. Consider $\mathbf{x} \in \mathbb{R}_+^p = [0, \infty)^p$, let t be a monotone bijection mapping from \mathbb{R} to \mathbb{R}_+ , with t^{-1} its inverse. For $\mathbf{y} \in \mathbb{R}^p$, $t(\mathbf{y})$ applies the transform componentwise. For \mathbf{x}_1 and $\mathbf{x}_2 \in \mathbb{R}_+^p = [0, \infty)^p$, define vector addition as $\mathbf{x}_1 \oplus \mathbf{x}_2 = t\{t^{-1}(\mathbf{x}_1) + t^{-1}(\mathbf{x}_2)\}$ and define scalar multiplication as $a \circ \mathbf{x}_1 = t\{at^{-1}(\mathbf{x}_1)\}$ for $a \in \mathbb{R}$. It is straightforward to show that \mathbb{R}_+^p with these transformed-linear operations is a vector space as it is isomorphic to \mathbb{R}^p with standard operations.

To apply transformed linear operations to non-negative regularly-varying random vectors, Cooley & Thibaud (2019) consider the softplus function $t(y) = \log\{1 + \exp(y)\}$. The important property is $\lim_{y \rightarrow \infty} t(y)/y = \lim_{x \rightarrow \infty} t^{-1}(x)/x = 1$. Because t negligibly affects large values, regular variation in the upper tail is preserved when t is used to define transformed-linear operations on regularly-varying random vectors. More precisely, if $sPr(b(s)^{-1}\mathbf{X}_i \in \cdot) \xrightarrow{v} \nu_{\mathbf{X}_i}(\cdot)$, $i = 1, 2$ and $\mathbf{X}_1, \mathbf{X}_2$ are independent, then $sPr(b(s)^{-1}(\mathbf{X}_1 \oplus \mathbf{X}_2) \in \cdot) \xrightarrow{v} \nu_{\mathbf{X}_1}(\cdot) + \nu_{\mathbf{X}_2}(\cdot)$; and $sPr[b(s)^{-1}(a \circ \mathbf{X}) \in \cdot] \xrightarrow{v} a^\alpha \nu_{\mathbf{X}}(\cdot)$ if $a > 0$, and $sPr[b(s)^{-1}(a \circ \mathbf{X}) \in \cdot] \xrightarrow{v} 0$ if $a \leq 0$. A lower tail condition is required which guarantees that $P(X_{i,j} < x) \rightarrow 0$ as $x \rightarrow 0$ fast enough so that when $a < 0$, $a \circ \mathbf{X}_i$ does not affect the upper tail. For the softplus t , the lower tail condition is $sPr\{X_{i,j} \leq \exp(-kb(s))\} \rightarrow 0$, as $s \rightarrow \infty$, $j = 1, \dots, p$, for all $k > 0$. The lower tail condition is met by common regularly varying distributions like the Fréchet and Pareto. Other $\mathbb{R} \mapsto \mathbb{R}_+$ transforms with the same limiting properties and with appropriately adjusted lower tail conditions could be used in place of t .

Cooley & Thibaud (2019) go on to construct $\mathbf{X} \in RV_+^p(\alpha)$ via transformed linear combinations of independent regularly varying random variables. Let $A = (\mathbf{a}_1, \dots, \mathbf{a}_q)$,

where $\mathbf{a}_j \in \mathbb{R}^p$ and hence $A \in \mathbb{R}^{p \times q}$. Let

$$\mathbf{X} = A \circ \mathbf{Z} = t(At^{-1}(\mathbf{Z})), \quad (2)$$

where $\mathbf{Z} = (Z_1, \dots, Z_q)^T$ is a vector of independent regularly varying random variables where $sPr(b(s)^{-1}Z_j > z) \rightarrow z^{-\alpha}$ for all j . \mathbf{X} is regularly varying with angular measure

$$H_{\mathbf{X}} = \sum_{j=1}^q \|\mathbf{a}_j^{(0)}\|^\alpha \delta_{\mathbf{a}_j^{(0)}/\|\mathbf{a}_j^{(0)}\|}(\cdot), \quad (3)$$

where δ is the Dirac mass function. The zero operation $a^{(0)} := \max(a, 0)$ will be important throughout, and is understood to be componentwise when applied to vectors or matrices. As $q \rightarrow \infty$ the class of angular measures resulting from this construction method is dense in the class of possible angular measures.

2.3 Tail Pairwise Dependence Matrix

If p is even moderately large, it is challenging to describe the angular measure $H_{\mathbf{X}}$ for $\mathbf{X} \in RV_+^p(\alpha)$. Rather than fully characterize $H_{\mathbf{X}}$, we will summarize tail dependence via a matrix of pairwise summary measures. Many bivariate dependence measures have been suggested for extremes; we choose one which has properties similar to covariance.

Let $\alpha = 2$ and let $\mathbf{X} \in RV_+^p(2)$ have angular measure $H_{\mathbf{X}}$. Let $\Sigma_{\mathbf{X}} = \{\sigma_{\mathbf{X}_{ij}}\}_{i,j=1,\dots,p}$ be the $p \times p$ matrix where

$$\sigma_{\mathbf{X}_{ij}} = \int_{\Theta_{p-1}^+} w_i w_j dH_{\mathbf{X}}(w), \quad (4)$$

and $\Theta_{p-1}^+ = \{\mathbf{w} \in \mathbb{R}_+^{p-1} : \|\mathbf{w}\|_2 = 1\}$. Each element $\sigma_{\mathbf{X}_{ij}}$ is essentially the extremal dependence measure of Larsson & Resnick (2012); however unlike Larsson & Resnick (2012), we require that $\alpha = 2$ and the L_2 norm which together make $\Sigma_{\mathbf{X}}$ have properties analogous to a covariance matrix. Specifically, $\Sigma_{\mathbf{X}}$ can be shown to be positive semi-definite (Cooley & Thibaud 2019). Following Cooley & Thibaud (2019), we call $\Sigma_{\mathbf{X}}$ the tail pairwise

dependence matrix. This should not be confused with the ‘tail dependence matrix’ of Shyamalkumar & Tao (2020) which is a matrix of alternate extremal dependence measures χ_{ij} (Coles et al. 1999) and which is not guaranteed to be positive definite.

Larsson & Resnick (2012) also assume $H_{\mathbf{X}}$ is a probability measure, giving their extremal dependence measure a fixed range of values analogous to correlation. We do not require $H_{\mathbf{X}}$ to be a probability measure, and like a covariance matrix the diagonal elements $\sigma_{\mathbf{X}ii}$ reflect the relative magnitudes of the respective elements X_i . Regular variation implies $\lim_{s \rightarrow \infty} sPr(b(s)^{-1}X_i > c) = c^{-2}\sigma_{\mathbf{X}ii}$. Letting $x = cU(s)s^{1/2}$, there is a corresponding slowly varying function such that the relation can be rewritten as

$$\lim_{x \rightarrow \infty} \frac{Pr(X_i > x)}{x^{-2}L(x)} = \sigma_{\mathbf{X}ii}. \quad (5)$$

So the ‘magnitude’ of the elements of \mathbf{X} described by the diagonal elements of the TPDM is in terms of suitably-normalized tail probabilities rather than variance. The presence of the slowly varying function $L(x)$ in the denominator means it is ambiguous to discuss the ‘scale’ of a regularly varying random variable, as scale information is in both the normalizing sequence and the angular measure (and consequently, TPDM). Because the notion of ‘scale’ is inherent in principal component analysis, Cooley & Thibaud (2019) further assumed that \mathbf{X} was Pareto-tailed, making $L(x)$ a constant that was pushed into the angular measure $H_{\mathbf{X}}$ and subsequently into $\Sigma_{\mathbf{X}}$. Here, we will not require a Pareto tail, and the random variables we will construct in Section 3 will have a natural normalizing function.

An additional property of the TPDM that is not generally true for covariance matrices is that it is completely positive. That is, there exists some $q_* < \infty$ and a nonnegative $p \times q_*$ matrix A_* such that $\Sigma_{\mathbf{X}} = A_*A_*^T$. The value of q_* is not known, and A_* is not unique.

If $\mathbf{X} = A \circ \mathbf{Z}$ as in (2), the TPDM of the resulting vector is $\Sigma_{A \circ \mathbf{Z}} = A^{(0)}A^{(0)T}$. Further, if $\mathbf{X} \in RV_+^p(2)$ has TPDM $\Sigma_{\mathbf{X}}$, the completely positive decomposition implies that there

exists a $0 < q_* < \infty$ and a nonnegative $p \times q_*$ matrix A_* such that $\mathbf{X}_* := A_* \circ \mathbf{Z}$ has the same TPDM as \mathbf{X} . In Section 5, we will use this completely positive decomposition to create prediction intervals.

3 Inner product space and prediction

3.1 Inner product space \mathcal{V}^q

We consider a space of regularly varying random variables constructed from transformed-linear combinations. We assume $\alpha = 2$ to obtain an inner product space. Let $\mathbf{Z} = (Z_1, \dots, Z_q)^T$ be a vector of independent $Z_j \in RV_+^1(2)$ meeting lower tail condition $sPr(b(s)^{-1}Z_j > z) \rightarrow z^{-2}$ and which have a common normalizing function $\lim_{z \rightarrow \infty} \frac{P(Z_j > z)}{z^{-2}L(z)} = 1$ for $j = 1, \dots, q$. For $\mathbf{a} \in \mathbb{R}^q$, consider the space

$$\mathcal{V}^q = \{X; X = \mathbf{a}^T \circ \mathbf{Z} = a_1 \circ Z_1 \oplus \dots \oplus a_q \circ Z_q\}. \quad (6)$$

$\mathcal{V}^q \subset RV_+^1(2)$. If $X_1 = \mathbf{a}_1^T \circ \mathbf{Z}$ and $X_2 = \mathbf{a}_2^T \circ \mathbf{Z}$, then $X_1 \oplus X_2 = (\mathbf{a}_1 + \mathbf{a}_2)^T \circ \mathbf{Z}$. Also, $c \circ X_1 = c\mathbf{a}_1 \circ \mathbf{Z}$ for $c \in \mathbb{R}$. \mathcal{V}^q is isomorphic to \mathbb{R}^q as any $X \in \mathcal{V}^q$ is uniquely identifiable by its vector of coefficients \mathbf{a} . Like \mathbb{R}^q , \mathcal{V}^q is complete and thus is a Hilbert space (Lee 2022). \mathcal{V}^q differs from the vector space in Cooley & Thibaud (2019) which was a non-stochastic vector space for \mathbb{R}_+^p .

We define the inner product of $X_1 = \mathbf{a}_1^T \circ \mathbf{Z}$ and $X_2 = \mathbf{a}_2^T \circ \mathbf{Z}$ as

$$\langle X_1, X_2 \rangle := \mathbf{a}_1^T \mathbf{a}_2 = \sum_{i=1}^q a_{1i} a_{2i}.$$

We say $X_1, X_2 \in \mathcal{V}^q$ are orthogonal if $\langle X_1, X_2 \rangle = 0$. The norm is defined as $\|\mathbf{X}\|_{\mathcal{V}^q} = \sqrt{\langle X, X \rangle}$, whose subscript \mathcal{V}^q distinguishes this norm based on the random variable's coefficients from the usual Euclidean norm. The norm defines a metric $d(X_1, X_2) = \|X_1 \ominus X_2\|_{\mathcal{V}^q}$.

We will further describe the meaning of this metric in Section 4.

We will consider vectors $\mathbf{X} = (X_1, \dots, X_p)^T$ where $X_i = \mathbf{a}_i^T \circ \mathbf{Z} \in \mathcal{V}^q$ for $i = 1, \dots, p$. $\mathbf{X} \in RV_+^p(2)$ and is of the form $A \circ \mathbf{Z}$ in (2). We denote the matrix of inner products

$$\Gamma_{\mathbf{X}} = \langle X_i, X_j \rangle_{i,j=1,\dots,p} = AA^T. \quad (7)$$

We will relate $\Gamma_{\mathbf{X}}$ for X_i in \mathcal{V}^q to the TPDM $\Sigma_{\mathbf{X}}$ for general $\mathbf{X} \in RV_+^p(2)$ in Section 4.

3.2 Transformed-linear prediction

As \mathcal{V}^q is isomorphic to Hilbert space \mathbb{R}^q , the best transformed-linear predictor follows similarly. Assume $X_i = \mathbf{a}_i^T \circ \mathbf{Z} \in \mathcal{V}^q$ for $i = 1, \dots, p+1$. Let $\mathbf{X}_p = (X_1, \dots, X_p)^T$. We aim to find $\mathbf{b} \in \mathbb{R}^p$ such that $d(\mathbf{b}^T \circ \mathbf{X}_p, X_{p+1})$ is minimized. Writing in matrix form

$$\begin{bmatrix} \mathbf{X}_p \\ X_{p+1} \end{bmatrix} = \begin{bmatrix} A_p \\ \mathbf{a}_{p+1}^T \end{bmatrix} \circ \mathbf{Z},$$

where $A_p = (\mathbf{a}_1^T, \dots, \mathbf{a}_p^T)^T$. The matrix of inner products of $(\mathbf{X}_p^T, X_{p+1})^T$ is

$$\Gamma_{(\mathbf{X}_p^T, X_{p+1})^T} = \begin{bmatrix} A_p A_p^T & A_p \mathbf{a}_{p+1}^T \\ \mathbf{a}_{p+1}^T A_p^T & \mathbf{a}_{p+1}^T \mathbf{a}_{p+1} \end{bmatrix} := \begin{bmatrix} \Gamma_{11} & \Gamma_{12} \\ \Gamma_{21} & \Gamma_{22} \end{bmatrix}. \quad (8)$$

Minimizing $d(\mathbf{b}^T \circ \mathbf{X}_p, X_{p+1})$ is equivalent to minimizing $\|A_p^T \mathbf{b} - \mathbf{a}_{p+1}\|_2^2$. Taking derivatives with respect to \mathbf{b} and setting equal to zero, the minimizer $\hat{\mathbf{b}}$ solves $(A_p A_p^T) \hat{\mathbf{b}} = A_p \mathbf{a}_{p+1}$. If $A_p A_p^T$ is invertible, then the solution $\hat{\mathbf{b}}$ is,

$$\hat{\mathbf{b}} = (A_p A_p^T)^{-1} A_p \mathbf{a}_{p+1} = \Gamma_{11}^{-1} \Gamma_{12}. \quad (9)$$

An equivalent way to think of the best transformed-linear prediction is through the projection theorem. \hat{X}_{p+1} is such that $X_{p+1} \ominus \hat{X}_{p+1}$ is orthogonal to the plane spanned by X_1, \dots, X_p . The orthogonality condition can be stated as $\langle X_{p+1} \ominus \hat{X}_{p+1}, X_i \rangle = 0$, for $i = 1, \dots, p$. By linearity of inner products, this can equivalently be expressed in matrix

notation as

$$\left[\langle X_{p+1}, X_i \rangle \right]_{i=1}^p = \left[\langle X_i, X_j \rangle \right]_{i,j=1}^p \left[b_i \right]_{i=1}^p = \left[\sum_{k=1}^q a_{ik} a_{jk} \right]_{i,j=1}^p \left[b_i \right]_{i=1}^p. \quad (10)$$

By (8), $\hat{\mathbf{b}}$ satisfies $A_p \mathbf{a}_{p+1} = A_p A_p^T \hat{\mathbf{b}}$ as above.

4 Subset \mathcal{V}_+^q

We have employed transformed linear operations to construct regularly-varying random vectors $\mathbf{X} = A \circ \mathbf{Z}$ that take values in the positive orthant, and we have tied these vectors' elements to the vector space \mathcal{V}^q . It is essential that the elements of the coefficient vectors \mathbf{a} are allowed to be negative for \mathcal{V}^q to be a vector space. However, negative values in \mathbf{a} do not influence tail behavior. Recalling that if regularly varying Z_1, Z_2 are independent, $P(Z_1 + Z_2 > z) \sim P(Z_1 > z) + P(Z_2 > z)$ as $z \rightarrow \infty$ (cf. Jessen & Mikosch 2006, Lemma 3.1), we can discuss the magnitude of $X \in \mathcal{V}^q$ (as in (5)) in terms of the common tail behavior of the generating Z_j 's. We call

$$TR(X) := \lim_{z \rightarrow \infty} \frac{P(X > z)}{P(Z_1 > z)} = \sum_{j=1}^q (a_j^{(0)})^2$$

the tail ratio of X and only the positive elements of \mathbf{a} contribute. $X = \mathbf{a} \circ \mathbf{Z} \in \mathcal{V}^q$ and $X_+ = \mathbf{a}^{(0)} \circ \mathbf{Z}$ have the same tail ratio. Furthermore, if $\mathbf{X} = A \circ \mathbf{Z}$, both it and $\mathbf{X}_+ = A^{(0)} \circ \mathbf{Z}$ have the same angular measure: $H_{\mathbf{X}} = H_{\mathbf{X}_+} = \sum_{j=1}^q \|a_j^{(0)}\|^2 \delta_{a_j^{(0)}/\|a_j^{(0)}\|}(\cdot)$. \mathbf{X} and \mathbf{X}_+ are indistinguishable in terms of their tail behavior.

In terms of modeling, it seems reasonable to restrict our attention to the subset $\mathcal{V}_+^q = \{X; X = \mathbf{a}^T \circ \mathbf{Z} = a_1 \circ Z_1 \oplus \cdots \oplus a_q \circ Z_q\}$, where $a_j \in [0, \infty)$, and $\mathbf{Z} = (Z_1, \dots, Z_q)^T$ as in (6). Considering inference for a random vector $\mathbf{X} \in RV_+^p$, we assume that $\mathbf{X} = A \circ \mathbf{Z}$ for some unknown $p \times q$ matrix A because it is a simple and useful modeling framework. Recall such constructions are dense in RV_+^p . Inference for \mathbf{X} will focus on its tail behavior,

and since this is indistinguishable from that of \mathbf{X}_+ , it is reasonable to assume $a_{ij} \geq 0$ for $i = 1, \dots, p$, and $j = 1, \dots, q$, and thus $X_i \in \mathcal{V}_+^q$ for $i = 1, \dots, p$.

Continuing with inference, if p is even of moderate size, then estimating $H_{\mathbf{X}}$ is challenging, so we focus on summarizing dependence via the TPDM. If $\mathbf{X} = A \circ \mathbf{Z}$ and all $a_{ij} \geq 0$, then $\Sigma_{\mathbf{X}} = \Gamma_{\mathbf{X}} = AA^T$. Furthermore, if inference focuses on the TPDM, then q , the number of independent Z_j 's from which \mathbf{X} is generated, does not need to be specified.

Turning our attention toward prediction, it seems reasonable to assume that the elements of $(\mathbf{X}_p^T, X_{p+1})^T$ are in \mathcal{V}_+^q , and prediction can be done in terms of the TPDM. Considering predictors of the form $\mathbf{b}^T \circ \mathbf{X}_p$ and letting $\Sigma_{(\mathbf{X}_p^T, X_{p+1})^T}$ be partitioned as in (8), $\hat{X}_{p+1} = \hat{\mathbf{b}}^T \circ \mathbf{X}_p$ where $\hat{\mathbf{b}} = \Sigma_{11}^{-1}\Sigma_{12}$ will minimize $\|X_{p+1} \ominus \hat{X}_{p+1}\|_{\mathcal{V}^q}$. Because $\hat{\mathbf{b}}$ is not required to consist of nonnegative elements, the predictor \hat{X}_{p+1} is not necessarily in \mathcal{V}_+^q .

We can now better discuss the meaning of the metric $d(X_1, X_2) = \|X_1 \ominus X_2\|_{\mathcal{V}^q}$, which in turn provides interpretation of what our predictor minimizes. Except under the unusual circumstance where $\sum_{j=1}^q ((a_{1j} - a_{2j})^{(0)})^2 = \sum_{j=1}^q ((a_{2j} - a_{1j})^{(0)})^2$, $TR(X_1 \ominus X_2)$ does not equal $TR(X_2 \ominus X_1)$. However, because $P(\max(Z_1, Z_2) > z) \sim P(Z_1 > z) + P(Z_2 > z)$ as $z \rightarrow \infty$,

$$TR(\max((X_1 \ominus X_2), (X_2 \ominus X_1))) = \sum_{j=1}^q (a_{1j} - a_{2j})^2 = d^2(X_1, X_2).$$

Thus $\hat{\mathbf{b}}$ is such that $TR(\max((X_{p+1} \ominus \hat{X}_{p+1}), (\hat{X}_{p+1} \ominus X_{p+1})))$ is minimized, and our best transformed linear predictor can be understood via this tail property rather than only in terms of the coefficients of \mathcal{V}^q , which are presumably unknown.

5 Prediction Error

5.1 Analogue to Mean Square Prediction Error

In the non-extreme setting, linear prediction minimizes MSPE. Additionally, as MSPE corresponds to the conditional variance under a Gaussian assumption, it is used to generate Gaussian-based prediction intervals. Our transformed linear prediction has an analogous quantity

$$\begin{aligned}
 \|\hat{X}_{p+1} \ominus X_{p+1}\|_{\mathcal{Y}^q}^2 &:= \langle \hat{X}_{p+1} \ominus X_{p+1}, \hat{X}_{p+1} \ominus X_{p+1} \rangle \\
 &= (\hat{\mathbf{b}}^T A_p - \mathbf{a}_{p+1}^T)(\hat{\mathbf{b}}^T A_p - \mathbf{a}_{p+1}^T)^T \\
 &= \Sigma_{22} - \Sigma_{21}\Sigma_{11}^{-1}\Sigma_{12} := K.
 \end{aligned} \tag{11}$$

Importantly, K can be calculated directly from the (estimated) TPDM. Unlike MSPE, K is not understood via expectation, but instead via tail probabilities as

$$TR\left(\max((X_{p+1} \ominus \hat{X}_{p+1}), (\hat{X}_{p+1} \ominus X_{p+1}))\right) = K.$$

The quantity K is meaningful to minimize, but seems not very useful for constructing prediction intervals. To illustrate, we simulate $n = 20,000$ four dimensional vectors \mathbf{X} and obtain \hat{X}_4 predicted on $(X_1, X_2, X_3)^T$. \mathbf{X} is generated from a 4×10 matrix A applied to a vector \mathbf{Z} comprised of 10 independent $RV_+(2)$ random variables; the elements of A are drawn from a uniform(0,5) distribution. Using the known TPDM to obtain $K = 0.224$ and known tail behavior of the Z_j 's, we calculate $P(D \leq 2.99) \approx 0.95$ where $D = \max((X_{p+1} \ominus \hat{X}_{p+1}), (\hat{X}_{p+1} \ominus X_{p+1}))$. We observe 0.952 of the simulated D values are in fact below this bound. However, Figure 2 shows that knowledge of K is not useful for constructing prediction intervals. Unlike the Gaussian case where the variance of the conditional distribution does not depend on the predicted value \hat{X}_{p+1} , in the polar geometry of regular variation, the magnitude of the error is related to the size of the predicted value.

In the next sections we use the polar geometry of regular variation to construct meaningful prediction intervals when \hat{X}_{p+1} is large.

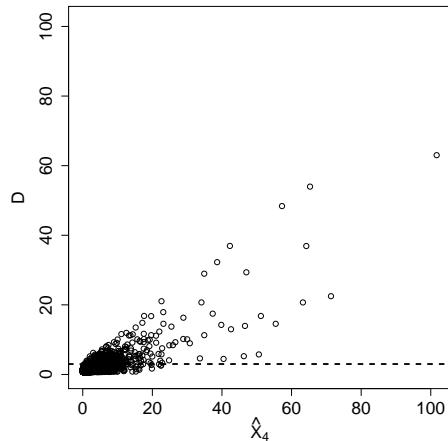


Figure 2: Left panel: The plot of $D = \max(\hat{X}_4 \ominus X_4, X_4 \ominus \hat{X}_4)$ against \hat{X}_4 . The horizontal dashed line indicates the approximate 0.95 quantile for D .

5.2 Prediction inner product matrix and completely positive decomposition

The vector $(\hat{X}_{p+1}, X_{p+1})^T \in RV_+^2(2)$, and this vector's tail dependence is characterized by $H_{(\hat{X}_{p+1}, X_{p+1})^T}$. While this angular measure is not readily available, the 2×2 ‘prediction’ inner product matrix

$$\Gamma_{(\hat{X}_{p+1}, X_{p+1})^T} = \begin{bmatrix} (\hat{\mathbf{b}}^T A_p) \\ \mathbf{a}_{p+1}^T \end{bmatrix} \begin{bmatrix} (A_p^T \hat{\mathbf{b}}) & \mathbf{a}_{p+1} \end{bmatrix} = \begin{bmatrix} \Sigma_{21} \Sigma_{11}^{-1} \Sigma_{12} & \Sigma_{21} \Sigma_{11}^{-1} \Sigma_{12} \\ \Sigma_{21} \Sigma_{11}^{-1} \Sigma_{12} & \Sigma_{22} \end{bmatrix}, \quad (12)$$

is readily available from the TPDM, and we use the information in this matrix to quantify prediction uncertainty. The last expression in (12) is in terms of the partitioned TPDM, as we have assumed $X_1, \dots, X_{p+1} \in \mathcal{V}_+^q$.

Although the entries of $\hat{\mathbf{b}}^T A_p$ are not guaranteed to be nonnegative, the Cholesky decomposition of the 2×2 prediction inner product matrix yields positive entries and thus

$\Gamma_{(\hat{X}_{p+1}, X_{p+1})^T}$ is completely positive. We use the non-uniqueness of completely positive decomposition to obtain nonnegative $2 \times q_*$ matrices B such that $BB^T = \Gamma_{(\hat{X}_{p+1}, X_{p+1})^T}$, and use (3) to construct a potential angular measure. Given a $q_* \geq 2$, there exist procedures (Groetzner & Dür 2020) to find examples of these matrices B . Since our goal is to obtain a potential angular measure $\hat{H}_{(\hat{X}_{p+1}, X_{p+1})^T}$ from the information in $\Gamma_{(\hat{X}_{p+1}, X_{p+1})^T}$, there would seem to be incentive to set q_* large, thereby distributing the total mass of the angular measure $H_{B \circ \mathbf{Z}}$ into q_* point masses. On the other hand, as q_* grows, the procedures for obtaining B require more computation. We take a practical approach. We choose q_* to be of moderate size, but apply the procedure repeatedly, obtaining nonnegative $B^{(k)}, k = 1, \dots, n_{decomp}$, such that $B^{(k)}B^{(k)T} = \Gamma_{(\hat{X}_{p+1}, X_{p+1})^T}$ for all k . We then set $\hat{H}_{(\hat{X}_{p+1}, X_{p+1})^T} = n_{decomp}^{-1} \sum_{k=1}^{n_{decomp}} H_{B^{(k)} \circ \mathbf{Z}}$, and $n_{decomp}^{-1} \sum_{k=1}^{n_{decomp}} B^{(k)}B^{(k)T} = \Gamma_{(\hat{X}_{p+1}, X_{p+1})^T}$ as desired. $\hat{H}_{(\hat{X}_{p+1}, X_{p+1})^T}$ consists of $n_{decomp}q_*$ point masses.

We use a simulation study to illustrate. We again begin by generating a matrix A whose elements are drawn from a uniform(0,5) distribution; however this time the dimension of A is 7×400 thus the true angular measure consists of 400 point masses. We draw 60,000 random realizations of $\mathbf{X} = A \circ \mathbf{Z}$, and use the first 40,000 as a training set. The largest 1% of this training set is used to estimate the seven-dimensional TPDM, from which we obtain $\hat{\mathbf{b}}$ and additionally $\hat{\Gamma}_{(\hat{X}_{p+1}, X_{p+1})^T}$. We then use the completely positive decomposition to obtain 2×9 matrices $B^{(k)}, k = 1, \dots, 51$, resulting in an estimated angular measure $\hat{H}_{(\hat{X}_{p+1}, X_{p+1})^T}$ consisting of 459 point masses. We obtain a 95% joint region by drawing bounds at the 0.025 and 0.975 quantiles of $\hat{H}_{(\hat{X}_{p+1}, X_{p+1})^T}$. The left panel of Figure 3 shows the scatterplot of the 20,000 remaining test points \hat{X}_{p+1} and X_{p+1} and the 95% joint region. Thresholding at the 0.95 quantile of $\|(\hat{X}_{p+1}, X_{p+1})\|_{\mathcal{V}^q}$, we find that 0.963 of the large values fall within the joint region.

5.3 Prediction intervals for X_{p+1} given large \hat{X}_{p+1}

The region obtained in the previous section describes the joint behavior of \hat{X}_{p+1} and X_{p+1} , but the quantity of interest is the conditional behavior of X_{p+1} given a specific large value of \hat{X}_{p+1} . Cooley et al. (2012) use the limiting intensity function of regular variation to get an approximate density of X_{p+1} given large \mathbf{X}_p . They fit a parametric model for $H_{(\mathbf{X}_p, X_{p+1})^T}$ and transform from polar form to obtain $\nu_{(\mathbf{X}_p, X_{p+1})^T}(d\mathbf{x})$. Cooley et al. (2012) applied their method in moderate dimension ($p = 4$). Applying their approach in higher dimensions would require fitting a high dimensional angular measure model. We adapt the method of Cooley et al. (2012) to model the relationship between X_{p+1} and \hat{X}_{p+1} . Regardless of p , we only need to describe this bivariate relationship.

Changing from polar coordinates to Cartesian, a bivariate regularly varying random vector (X_1, X_2) with $\alpha = 2$ and angular density $h_{(X_1, X_2)}$ defined on Θ_1^+ has limiting measure $\nu(dx_1, dx_2) = 2\|\mathbf{x}\|_2^{-5}x_2h(\mathbf{x}\|\mathbf{x}\|_2^{-1})$. Following Cooley et al. (2012), the conditional density of $X_2|X_1 = x_1$ if x_1 is large is approximately

$$f_{X_2|X_1}(x_2|x_1) = 2c^{-1}\|(x_1, x_2)\|_2^{-5}x_2h\left(\frac{(x_1, x_2)}{\|(x_1, x_2)\|_2}\right), \quad (13)$$

where $c = \int_0^\infty 2\|(x_1, x_2)\|_2^{-5}x_2h\left(\frac{(x_1, x_2)}{\|(x_1, x_2)\|_2}\right) dx_2$.

We use (13) to obtain an estimate of the conditional density of X_{p+1} given large \hat{X}_{p+1} . Since (13) requires an angular density, we use a kernel density estimate of $\hat{H}_{(\hat{X}_{p+1}, X_{p+1})^T}$. We use the adjusted boundary bias approach of Marron & Ruppert (1994) for the kernel density estimation since the support of $H_{(\hat{X}_{p+1}, X_{p+1})}$ is bounded. We then take the 0.025 and 0.975 quantiles of this estimated conditional density to obtain a 95% prediction interval. The center panel of Figure 3 illustrates the conditional density for a particular realization from the aforementioned simulation study where $\hat{X}_{p+1} = 33.17$ and with actual value $X_{p+1} = 48.15$ denoted by the blue star. The right panel shows a scatterplot of the largest 5% (by

\hat{X}_{p+1}) of the test set from the aforementioned simulation along with the upper and lower bounds from the conditional density approximation. The coverage rate of these intervals is 0.947.

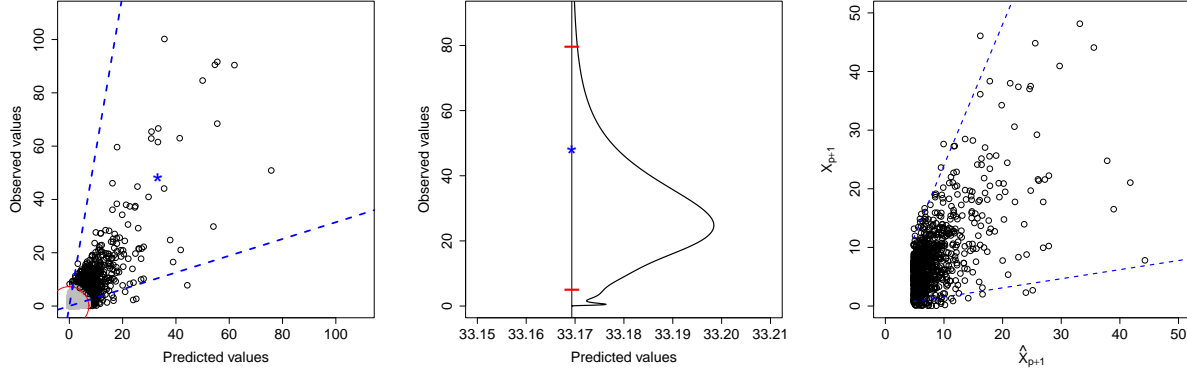


Figure 3: (Left) The estimated joint 95% joint prediction region based on the approximated angular measure $\hat{H}_{(\hat{X}_{p+1}, X_{p+1})^T}$. The star indicates a particular observation which has a predicted value of 33.17 and an observed value of 48.15. (Center) The approximate conditional density $f_{X_{p+1}|\hat{X}_{p+1}}(X_{p+1}|\hat{x}_{p+1} = 33.17)$. The horizontal segments indicate the 95% conditional prediction interval, and the star denotes the actual value of 48.15. The units of the horizontal axis are the predicted values and the units of the conditional density are omitted. (Right) the scatter plot of \hat{X}_{p+1} and X_{p+1} with 95% conditional prediction intervals given each large value of \hat{X}_{p+1} .

6 Applications

6.1 Nitrogen dioxide air pollution.

NO₂ is one of six air pollutants for which the US Environmental Protection Agency (EPA) has national air quality standards. We analyze daily EPA NO₂ data¹ from five locations

¹<https://www.epa.gov/outdoor-air-quality-data/download-daily-data>

in the Washington DC metropolitan area (see Figure 1). The first four stations (McMillan 11-001-0043, River Terrace 11-001-0041, Takoma 11-001-0025, Arlington 51-013-0020) have long data records spanning 1995-2020. Alexandria does not have observations after 2016. We will perform prediction at Alexandria given data at the other four locations. Observations in Alexandria actually come from two different stations: 51-510-0009 which has measurements from January 1995 to August 2012 and 51-510-00210 from August 2012 to April 2016. Exploratory analysis did not indicate any detectable change point in the Alexandria data either with respect to the marginal distribution or with dependence with other stations, so we treat this data as coming from a single station. There are 5163 days between 1995 and 2016 where all five locations have measurements. Because NO_2 levels have decreased over the study period, we detrend at each location using a moving average mean and standard deviation with window of 901 days to center and scale.

Our inner product space assumes each $X_i \in RV_+^1(\alpha = 2)$, and the detrended NO_2 data must be transformed to meet this assumption. In fact, it is unclear whether the NO_2 data are even heavy tailed. Nevertheless, we believe the regular variation framework is useful for describing the tail dependence for this data after marginal transformation. Characterizing dependence after marginal transformation is justified by Sklar's theorem (Sklar (1959), see also Resnick (1987, Proposition 5.15)), and such transformations are regularly used in multivariate extremes studies. After viewing standard diagnostic plots, we fit a generalized Pareto distribution above each location's 0.95 quantile and obtain the marginal estimated cdf's \hat{F}_i which are the empirical cdf below the 0.95 quantile and the fitted generalized Pareto above. Letting $X_i^{(orig)}$ denote the random variable for detrended NO_2 at location i , we define $X_i = 1/\sqrt{(1 - \hat{F}_i(X_i^{(orig)}))} - \delta$ obtaining a 'shifted' Pareto distribution for $i = 1, \dots, 5$. Each $X_i \in RV_+(\alpha = 2)$ and the shift $\delta = 0.9352$ is such that $E[t^{-1}(X_i)] = 0$.

This shift makes the preimages of the transformed data centered which we found reduced bias in the estimation of the TPDM. We assume $\mathbf{X} = (X_1, \dots, X_5)^T \in RV_+^5(\alpha = 2)$. Further, we let \mathbf{X}_t denote the random vector of observations on day t , which we assume to be iid copies of \mathbf{X} . This is a simplifying assumption as there is temporal dependence in the NO₂ data, but it seems less informative that the spatial dependence exhibited by each day's observations.

We first predict during the period prior to 2015 in order that we can use the observed data at Alexandria to assess performance. Indices are randomly drawn to divide the data set into training and test sets consisting of 3442 and 1721 observations respectively, and both sets cover the entire observational period. Using the training set, the five-dimensional TPDM $\hat{\Sigma}_{\mathbf{X}}$ is estimated as follows. Let \mathbf{x}_t denote the observed measurements on day t . For each $i \neq j$ in $1, \dots, 5$, let $r_{t,ij} = \|(x_{t,i}, x_{t,j})\|_2$ and $(w_{t,i}, w_{t,j}) = (x_{t,i}, x_{t,j})/r_{t,ij}$. We let $\hat{\sigma}_{ij} = 2n_{exc}^{-1} \sum_{t=1}^n w_{t,i}w_{t,j} \mathbb{I}(r_{t,ij} > r_{ij}^*)$, where $n_{exc} = \sum_{t=1}^n \mathbb{I}(r_{t,ij} > r_{ij}^*)$. We choose r_{ij}^* to correspond to the 0.95 quantile. The constant 2 arises from knowledge that the tail ratio of each X_i is one due to the marginal transformation. This pairwise estimation of the TPDM differs from the method in Cooley & Thibaud (2019) who used the entire vector norm as the radial component. Mhatre & Cooley (2021) show that the TPDM is equivalent whether it is defined in terms of the angular measure of the entire vector or the angular measure corresponding to the two-dimensional marginals.

From $\hat{\Sigma}_{\mathbf{X}}$, we obtain $\hat{X}_{t,5} = \hat{\mathbf{b}}^T \circ \mathbf{X}_{t,4}$, where $\hat{\mathbf{b}} = (-0.047, 0.177, 0.192, 0.482)^T$. We note that the largest weighted component is Arlington, which is closest to Alexandria. Interestingly, McMillan has a slightly negative weight. We calculate $\hat{X}_{t,5}$ for all t , but only consider those for which $\hat{X}_{t,5}$ exceeds the 0.95 quantile. The left panel of Figure 4 shows the scatterplot of the values $x_{t,5}$ versus $\hat{x}_{t,5}$. By taking the inverse of the marginal

transformation, multiplying by the moving average standard deviation and adding the moving average mean, the predicted value can be put on the scale of the original data. The center panel of Figure 4 shows the scatterplot on the original scale.

For each large predicted value $\hat{x}_{t,5}$, we use the method described in Section 5.3 to create 95% prediction intervals. We chose the matrix B arising from the completely positive decomposition to again be 2×9 . On the Pareto scale, these prediction intervals are linear with $\hat{x}_{t,5}$ and are shown in the left panel of Figure 4. The coverage rate of these intervals is 0.965. The intervals can similarly be back-transformed to be on the original scale as shown in the center panel of Figure 4. The lack of monotonicity in these intervals with respect to the predicted value is due to the trend in the data over the observation period.

For comparison to standard linear prediction, we find the BLUP based on the estimated covariance matrix from the entire data set, and create Gaussian-based 95% confidence intervals from the estimated MSPE. When done on the original data, we obtain a coverage rate of 0.88, and when done on square-root transformed data to account for the skewness, we obtain a coverage rate of 0.78.

We also compare our prediction method to the extremes-based method of Cooley et al. (2012), which approximated the conditional distribution of the large values of a regularly varying variate via a parametric model for the angular measure. The method of Cooley et al. (2012) can be done due to this application's relatively low dimension. As done in Cooley et al. (2012), the pairwise beta model (Cooley et al. 2010) is fit by maximum likelihood to the preprocessed training data set. The 95% prediction intervals are based on the approximated conditional density of X_5 given x_1, \dots, x_4 , and the achieved coverage rate for the test set is 0.965. Because the fitted angular measure model would seemingly contain more information than the estimated TPDM, we were surprised that the widths of

the prediction intervals were very similar for the two methods. The average ratio of Cooley et al. (2012) average interval width to our TPDM-based approach was 1.04.

We then apply our prediction method to five dates in 2019 and 2020 when observed values at the four recording stations were large and no observation was taken at Alexandria. Here, we use the entire period from 1995-2016 to estimate the TPDM, and we obtain a slightly different estimate $\hat{\mathbf{b}} = (0.026, 0.153, 0.118, 0.461)^T$. The right panel of Figure 4 shows the point estimate and 95% prediction intervals from our transformed-linear approach (after back transformation to original scale). The trend at Arlington was used for the unobserved trend at Alexandria. For comparison, covariance matrix-based BLUP's and MSPE-based 95% prediction intervals for these dates are shown with a dashed line.

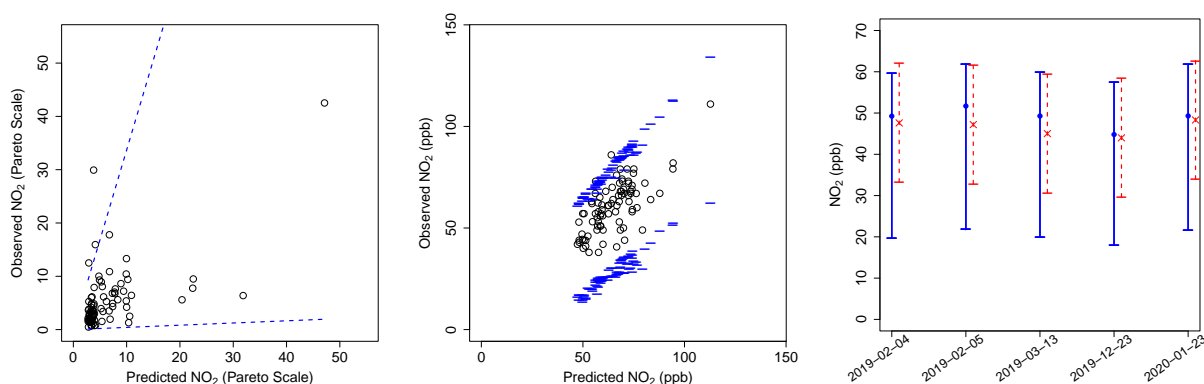


Figure 4: (Left) Scatterplot of \hat{X}_5 and X_5 with the 95% prediction intervals on the Pareto scale. (Center) Scatterplot and 95% prediction intervals after transformation back to the original scale of the NO_2 data. (Right) Comparison of the point predictions and 95% prediction intervals using the transformed linear approach (solid line) and a Gaussian-based approach with the covariance matrix (dashed line) for five recent dates when Alexandria is not observed.

6.2 Industry portfolios.

We apply the transformed-linear prediction method to a higher dimensional financial data set. The data set obtained from the Kenneth French Data Library² contains the value-averaged daily returns of 30 industry portfolios. We analyze data for 1950-2020, consisting of $n = 17911$ observations. Since our interest is in extreme losses, we negate the returns, set negative returns to zero so that data is in the positive orthant. Although these data appear to be heavy-tailed, it still requires marginal transformation so that $\alpha = 2$ can be assumed. Let $\mathbf{X}^{(orig)}$ denote the random vector of the value-averaged daily returns. For simplicity we use the empirical CDF to perform the marginal transformation $X_i = 1/\sqrt{(1 - \hat{F}_i(X_i^{(orig)}))} - \delta$, which is applied to each industry's data so that X_i follows the same shifted Pareto distribution as before. We again assume \mathbf{X}_t , the random vector denoting the observations on day t , are iid copies of \mathbf{X} . The data set is randomly split into two sets. The training set consists of two-thirds of the data ($n_{train} = 11940$) to estimate the TPDM and obtain the vector $\hat{\mathbf{b}}$. The test set consists of the remaining one-third of the data ($n_{test} = 5970$) to assess coverage rates.

Following similar steps in the previous application, the 30×30 TPDM $\Sigma_{\mathbf{X}}$ is estimated first in the training set. We focus on performing the linear prediction for extreme losses of coal, beer, and paper. The three largest coefficients in $\hat{\mathbf{b}}_{coal}$ are $(0.42, 0.36, 0.20)$ and correspond to fabricated products and machinery, steel, and oil respectively. The three largest coefficients $\hat{\mathbf{b}}_{beer}$ are $(0.52, 0.24, 0.12)$ and correspond to food products, retail, and consumer goods (household). The three largest coefficients for $\hat{\mathbf{b}}_{paper}$ are $(0.21, 0.11, 0.08)$ and correspond to chemicals, consumer goods (household), and construction materials. The assessed coverage rates of our transformed linear 95% prediction intervals for coal, beer,

²https://mba.tuck.dartmouth.edu/pages/faculty/ken.french/data_library.html

and paper are 97.9%, 96.3%, and 98%, respectively.

For the purpose of comparison, we also assessed coverage rates of the MSPE-based 95% prediction intervals. Because the data are strongly non-Gaussian, we use the empirical CDF to transform the marginals to be standard normal before estimating the covariance matrix. The coverage rates of MSPE-based 95% prediction intervals are 79.3%, 66.6%, and 51.2% for coal, beer, and paper respectively.

7 Summary and Discussion

We have proposed a method for performing linear prediction when observations are large. To do so, we constructed an inner product space of nonnegative random variables arising from transformed linear combinations of independent regularly varying random variables. The elements of the TPDM correspond to these inner products if one is willing to assume that these random variables in \mathcal{V}_+^q . The projection theorem yields the optimal transformed linear predictor. Our method for obtaining prediction intervals shows very good performance both in a simulation study and in two applications. The method is simple and is based only on the TPDM which is estimable in high dimensions.

We restrict to nonnegative regularly varying random variables to focus attention on the upper tail. Relaxing this restriction could allow one to use standard linear operations. Even when the data can be negative, we believe there is value in focusing in one direction. In the financial application, tail dependence for extreme losses can be different than for gains, and this information is lost when dependence is summarized with a single number as in the TPDM.

The random vectors $\mathbf{X} = A \circ \mathbf{Z}$ comprised of elements of our vector space have a simple angular measure consisting of q point masses where q is the number of columns of

A. Previous models with angular measures consisting of discrete point masses have been criticized as being overly simple. A difference here is that we do not have to specify q to use this framework to perform prediction, or more generally, we do not have to really believe that our data arise from such a simple model. Rather, if we are comfortable with the information contained in the TPDM, then we can use its information to easily obtain a point prediction and sensible prediction intervals that reflect the information contained.

In many applications, dependence cannot be measured between the observed values and the value to be predicted. In kriging for example, a spatial process model is first fit so that covariance between any two locations is quantified. One can imagine modeling the extremal pairwise dependence as a function of distance before applying the methods here to perform prediction for extreme levels.

References

- Coles, S., Heffernan, J. & Tawn, J. (1999), ‘Dependence measures for extreme value analysis’, *Extremes* **2**, 339–365.
- Cooley, D., Davis, R. A. & Naveau, P. (2010), ‘The pairwise beta distribution: A flexible parametric multivariate model for extremes’, *Journal of Multivariate Analysis* **101**(9), 2103–2117.
- Cooley, D., Davis, R. A. & Naveau, P. (2012), ‘Approximating the conditional density given large observed values via a multivariate extremes framework, with application to environmental data’, *The Annals of Applied Statistics* **6**(4), 1406–1429.
- Cooley, D. & Thibaud, E. (2019), ‘Decompositions of dependence for high-dimensional extremes’, *Biometrika* **106**(3), 587–604.

- De Haan, L. & Ferreira, A. (2007), *Extreme value theory: an introduction*, Springer Science & Business Media.
- Groetzner, P. & Dür, M. (2020), ‘A factorization method for completely positive matrices’, *Linear Algebra and its Applications* **591**, 1–24.
- Jessen, H. A. & Mikosch, T. (2006), ‘Regularly varying functions’, *Publications de L’institut Mathématique* **80**(94), 171–192.
- Larsson, M. & Resnick, S. I. (2012), ‘Extremal dependence measure and extremogram: the regularly varying case’, *Extremes* **15**(2), 231–256.
- Lee, J. (2022), Linear prediction and partial tail correlation for extremes, PhD thesis, Colorado State University.
- Marron, J. S. & Ruppert, D. (1994), ‘Transformations to reduce boundary bias in kernel density estimation’, *Journal of the Royal Statistical Society: Series B (Methodological)* **56**(4), 653–671.
- Mhatre, N. & Cooley, D. (2021), ‘Transformed-linear models for time series extremes’.
- Resnick, S. I. (1987), *Extreme values, regular variation and point processes*, Springer.
- Resnick, S. I. (2007), *Heavy-tail phenomena: probabilistic and statistical modeling*, Springer Science & Business Media.
- Shyamalkumar, N. D. & Tao, S. (2020), ‘On tail dependence matrices’, *Extremes* pp. 1–41.
- Sklar, M. (1959), ‘Fonctions de repartition an dimensions et leurs marges’, *Publ. inst. statist. univ. Paris* **8**, 229–231.